*Final Draft*
**of the original manuscript:**

Onken, R.; Riethmueller, R.:
**Determination of the freshwater budget of tidal flats from measurements near a tidal inlet**
In: Continental Shelf Research ( 2010) Elsevier

DOI: 10.1016/j.csr.2010.02.004

# Determination of the freshwater budget of tidal flats from measurements near a tidal inlet

by
**Reiner Onken and Rolf Riethmüller**

Institute of Coastal Research
GKSS Research Centre
Max-Planck-Straße 1
21052 Geesthacht
Germany

$2^{nd}$ draft

February 8, 2010

# Abstract

The freshwater budget of a tidal flat area is evaluated from long-term hydrographic time series from an observation pole positioned in a tidal channel in the Hörnum Basin (Germany). For each tidal cycle, the freshwater budget is calculated from the total imported and exported water volumes and the corresponding mean densities. The variability of the budget on a tidal scale is characterised by a period of twice the tidal period, exhibiting a minimum when the tidal flats are dry around daylight hours during the foregoing low tide, and a maximum when low tide occurs at night; enhanced evaporation on the flats at daylight hours is identified as the driving process. On the average over one year, while winter observations are missing, the freshwater budget is negative for the years 2002–2005 and positive only for 2006. The interannual mean is negative and amounts to a freshwater loss of about 2 mm/day, although the large-scale climate in this region is humid. The results demonstrate that the bulk parametrisations for the latent and sensible heat flux between the ocean and the atmosphere must not be applied for the tidelands.



**Keywords**: Germany; German Bight; Wadden Sea; tidal flat; freshwater budget; tideland; evaporation


# 1 Introduction

A method is presented to obtain estimates of the freshwater budget of tidal flat areas from point measurements. The method is generalised in a way that it can be applied to any tidal basin: it is only necessary to measure the total water volumes and the corresponding mean densities entering and leaving the basin through the tidal inlet during flood and ebb, respectively.

The long-term mean freshwater budget of a semi-enclosed basin under the assumption that the mean sea level is constant, reads

$$\mathcal{O} - \mathcal{I} = \mathcal{P} - \mathcal{E} + \mathcal{M} - \mathcal{F} + \mathcal{R} \tag{1}$$

(all quantities except for $\mathcal{E}$ are positive; e.g. Dietrich et al., 1980). Here, on the right–hand side (*rhs*) of (1), $\mathcal{P}$ is the water gain by precipitation, $\mathcal{E}$ the loss/gain by evaporation/condensation, $\mathcal{M}$ and $\mathcal{F}$ are gains and losses of water by melting and freezing of ice, respectively, $\mathcal{R}$ is the land runoff by rivers and the entry of groundwater. These terms are balanced by $\mathcal{O} - \mathcal{I}$ on the left–hand side (*lhs*), representing the inflow $\mathcal{I}$ and the outflow $\mathcal{O}$ from and to the open ocean. The basin will be considered ice-free ($\mathcal{M} - \mathcal{F} = 0$), hence the *rhs* budget can simply be obtained from measurements of the *lhs* budget $\mathcal{O} - \mathcal{I}$.

For atmospheric forecast models, the knowledge of the latent and sensible heat fluxes at the lower boundary of the atmosphere (i.e. at the air/land or air/sea interface) are mandatory in order to predict convective events correctly. Over sea, those fluxes are parameterised in terms of the sea surface temperature and the wind speed, while over land additional information on the soil moisture is desirable (Maxwell et al., 2007). A special problem arises in the Wadden Sea areas which at low tide exhibit characteristics both of the open sea and land. In the past, this effect might have been negligible, but presently the resolution of the forecast models is approaching the 1-km scale (Neunhäuserer et al., 2007) and the objective of developers is to predict local weather phenomena correctly, e.g. land/sea breeze, squall lines, thunderstorms, or fog. Therefore, it is necessary to adequately parametrise the thermodynamic processes in the Wadden Sea.

The only publication known to the authors which investigates the water budget of a tidal flat area is that of Ridd et al. (1997) who studied the budget of a tidal salt flat in dry tropical Australia. As the contribution by precipitation was negligible at this site, only evaporation, the loss of salt by horizontal advection, and the salt accumulation in the groundwater were determined. While the mean evaporative loss of freshwater was about 3.5 mm/day, the gain of freshwater by groundwater entry was estimated as 1 mm/day. This net loss caused the average salt concentration of the ebb flow to be higher than that of the flood water. Other studies of tropical tidal flats (Wolanski and Ridd, 1986; Hollins and Ridd, 1997; Hughes et al., 2001) focussed on the trapping of high and low salinity water in mangrove swamps (Wolanski and Ridd, 1986). Hollins and Ridd (1997) observed a clear diurnal signal of evaporation with maximum evaporation during daylight hours. Hughes et al. (2001) measured directly the evapotranspiration (that includes the evaporation from plants) for a salt marsh and arrived at values between 2.5 mm/day and 4.5 mm/day. At moderate latitudes in New Zealand, Heath (1977) estimated an evaporation rate of 2.7 mm/day over a tidal mudflat from radiation measurements. By long-term measurements of Acreman et al. (2003) the evaporation rate on wet grassland and reed beds in southwest England was determined to about 2 mm/day. Finally, Rouse et al. (1992) obtained 4 mm/day for the evapotranspiration at a subarctic, wetland tundra site of the Hudson Bay Lowlands.

This paper is a follow-up study of Onken et al. (2007, to be referred to as OCVR07), who described a method to determine the heat budget of a tidal flat area in the Hörnum tidal basin (German Wadden Sea). A similar method is applied herein for the freshwater budget of the basin.

# 2 Geographic and oceanographic setting, observations

The Hörnum Basin (Fig. 1) covers an area of about 300 km$^2$. It is connected to the North Sea by three tidal inlets, the Hörnum Deep between Sylt and Amrun and two gaps between the Hörnum Basin and the Norderaue, one between the islands of Föhr and Amrun and one between Föhr and the mainland, referred to as the Föhr Shoulder. While the Hörnum Deep reaches a depth of more than 30 m close to the southern tip of Sylt, the other gaps are very shallow and are only submerged during high tide. Therefore, the major exchange of water with the open sea occurs through the Hörnum Deep. Here, the tidal prism is of the order of $10^6$ m$^3$; being one order of magnitude less for the shallow inlets (Ross et al. 1998). A special feature of the latter is that they are feeding water into the Hörnum Basin during flood, whereas the return flow from the Hörnum Basin during ebb is not significant. Hence, the residual water transport in the shallow inlets is directed north into the Hörnum Basin and the export volume through the Hörnum Deep is larger than the import volume.

Long term observations of oceanic and atmospheric parameters are underway at an observation pole in the Hörnum Deep marked in Fig. 1; the pole has been in operation since 2002 during the ice-free season from about March to November. Except for the water level, oceanic parameters are collected approximately 1 m above the bed by standard oceanographic sensors for pressure, temperature, and conductivity. Velocity is measured by two instruments: a Nortek ADV (Acoustic Doppler Velocimeter) records the velocity components at a fixed location below the instrument, while a horizontal RD Instruments Acoustic Doppler Current Profiler (ADCP, to be referred to as pADCP hereafter) measures the lateral structure of the velocity field over a distance of 71 m resolved into 14

bins of 5-m width each. The first bin is centred at 3.5 m to the side of the pole and covers the interval between 1 m and 6 m. Additional parameters collected routinely are transmittance and turbidity, and for a short time fluorescence, pH, and oxygen. The data of all instruments are sampled at high frequency, but because of the limited bandwidth of the cellphone communication the data are first averaged over ten minutes and the averages are sent to the GKSS database. However, a rapid two-Hertz sampling mode may be enabled for a short period of time to record special events.

For budget calculations it is necessary to convert the single-point measurements of velocity into volume fluxes within the tidal channel. To accomplish that a one-time survey with a ship mounted ADCP onboard RV "Ludwig Prandtl" was conducted in spring 2004 in the vicinity of the pole, continually crossing the Hörnum Deep back and forth from one bank to the other, and recording the surface to bottom volume flux for each crossing. In order to establish a relationship between the instantaneous volume flux $v(t)$ and the simultaneous velocity records at the pole at any time $t$, a linear regression

$$v(t) = a_0 + a_1\ u(t), \tag{2}$$

was performed, where where $a_0$=-354.1 $\mathrm{m^3 s^{-1}}$ , $a_1$=28265.3 $\mathrm{m^2}$, and $u(t)$ is the east velocity component of the first bin of the pADCP. The regression is then applied to all pADCP records since 2002, and a multi-year timeseries of the volume flux at the pole is obtained (for a more detailed description see OCVR07).

# 3 The freshwater budget of the Hörnum tidal basin

Fig. 2 shows the typical situation of a tidal basin in the Wadden Sea, that is situated between the mainland and an offshore island chain. The major exchange of sea water with the North Sea occurs through a tidal inlet between two islands and with the neighbouring basins across the water sheds. Sources and sinks of (water) mass exchanged within one tidal cycle between two successive low tides are indicated by the symbol $M$. The index $i$ designates **i**mported mass during the flood, while **e**xport during the ebb is indicated by the index $e$. Finally, $M_f$ is the **f**resh water surplus/deficit due to land runoff, precipitation, evaporation and condensation. In the following, evaporation and condensation will be referred to as "evaporation", which may be either negative or positive. Condensation effects are disregarded because they are assumed to be negligible.

In the most general case, the conservation of mass requires

$$\sum_{n=1}^{3} (M_{i,n} + M_{e,n}) + M_f + \epsilon_1 = 0, \tag{3}$$

where the imported quantities are treated as positive quantities (gain of mass) and the exported ones are negative (losses); $M_f$ may attain either sign – it is positive in the case of $\mathcal{P} + \mathcal{R} > \mathcal{E}$ or otherwise negative. $\epsilon_1$ accounts for the different water levels of successive low tides due to changing weather conditions, or the inequality of the tides.

If (3) is applied to the position of the pole in the Hörnum Basin, then index 1 indicates the mass exchanges in the channel occupied by the pole, index 2 denotes the transport over the Föhr Shoulder, and index 3 refers to the contribution through the gap between Amrum and Föhr. As the latter is outside the catchment area of the pole, $M_{i,3}$ and $M_{e,3}$ are considered as to be included in $M_{i,1}$ and $M_{e,1}$, respectively. Moreover, as $|M_{i,2}| >> |M_{e,2}|$(Ross et al. 1998), the approximation $M_{e,2} = 0$ appears appropriate and $M_{i,2}$ denotes

the net inflow over the Föhr Shoulder into the basin. An additional issue arises due to the fact that at high tide the cross section of the channel at the pole is not bounded by land; namely, water entering the basin during flood is confined to the channel, but the ebb trajectories may be on the lateral flats, thus the corresponding water parcels do not pass the pole. This uncertainty is expressed by $\epsilon_2$. In total, the fresh water budget in the catchment area of the pole reads as

$$M_f \approx -\left(M_{e,1} + M_{i,1} + M_{i,2} + \epsilon_1 + \epsilon_2\right). \tag{4}$$

Due to the shallow water depth between ≈3m at low tide and ≈5.5m at high tide and the strong tidal currents of up to 80 cm $s^{-1}$ , the water column is fully mixed at almost any time of the year. Then, the masses $M$ on the *rhs* may be expressed by their volumes $V$ and the corresponding volume weighted mean densities $\overline{\rho}$ (see (13), (14) below):

$$M_f \approx -\left(\overline{\rho}_{e,1}V_{e,1} + \overline{\rho}_{i,1}V_{i,1} + \overline{\rho}_{i,2}V_{i,2} + \epsilon_1 + \epsilon_2\right). \tag{5}$$

Now, because no observations are available, it is postulated that

$$\overline{\rho}_{i,1} = \overline{\rho}_{i,2} \equiv \overline{\rho}_i, \tag{6}$$

i.e. the densities of the incoming water masses at the pole and over the Föhr Shoulder are equal. This postulate is justified because the water masses entering the basin through the Hörnum Deep and the Norderaue originate both from the open North Sea, and it is legitimate to assume that their initial characteristics are identical. Moreover, as there is no significant contribution of freshwater inflow by riverine discharge along the tidal inlets, the salinity (and therefore the potential density) is assumed to be constant. $M_f$ is substituted by $\overline{\rho}_f V_f$, where $V_f$ is the volume of the freshwater budget and $\overline{\rho}_f$ its mean density. Then, after dropping the index of $V_{e,1}$, (5) reads as

$$\overline{\rho}_f V_f \approx -\left[\overline{\rho}_i\left(V_{i,1} + V_{i,2}\right) + \overline{\rho}_e V_e + \epsilon_1 + \epsilon_2\right]. \tag{7}$$

Analogously to the mass budget (3), the imported volumes may be expressed as

$$V_{i,1} + V_{i,2} \approx -V_f - V_e. \tag{8}$$

(Formally correct and in accordance with the mass budget, there should also appear two additional terms $\epsilon_3$ and $\epsilon_4$ in (8); these, however were neglected from the outset because they would later appear only as addends to $\epsilon_1$ and $\epsilon_2$, respectively). Substituting (8) in (7) and after some re-arrangement, the budget of the freshwater *volume* finally reads as

$$V_f \approx V_e\frac{\overline{\rho}_i - \overline{\rho}_e}{\overline{\rho}_f - \overline{\rho}_i} - \frac{\epsilon_1 + \epsilon_2}{\overline{\rho}_f - \overline{\rho}_i}. \tag{9}$$

In order to estimate the magnitude of $\epsilon_2$, trajectories of water particles in the channel were calculated with a numerical model (for details of the model see OCVR07). The results indicate that the fraction of particles entering the basin in the channel during flood and leaving the basin "through the back-door", i.e. over the tidal flats away from the pole, is not significant. Hence, $\epsilon_2 \equiv 0$ has been used. By contrast, $\epsilon_1 \neq 0$ for individual tides, but it is assumed that this error is small when $V_f$ is averaged over many tidal cycles, e.g. over one tropical month for removal of the fortnightly inequality. Then, the mean freshwater volume budget reads as

$$\overline{V}_f \approx V_e\frac{\overline{\rho}_i - \overline{\rho}_e}{\overline{\rho}_f - \overline{\rho}_i}. \tag{10}$$

For the present task, one is not interested in thermal variations of the density, hence all densities may be considered as potential densities referred to 0°C. If so, $\overline{\rho}_f \approx 1000$ kg m$^{-3}$ is a constant, and the denominator of (10) is always negative. The simplicity of (10) is striking, since $V_f$ is only a function of $V_e$ and the density difference of the exported water volumes. One should note, however, that $V_i$ is implicitly contained in $\overline{\rho}_i$. The equation indicates that the sign of $V_f$ is controlled just by the density difference: if $\overline{\rho}_e > \overline{\rho}_i$ , then the exported water mass is denser than the imported one; in that case, $V_f$ is negative, because $V_e < 0$ by definition and $\overline{\rho}_f - \overline{\rho}_i < 0$. $V_f < 0$ means a net loss of freshwater in the catchment area caused by evaporation overcompensating the freshwater input by precipitation and land runoff, hence during one tidal cycle, the imported freshwater volume is greater than the exported volume (import situation). Alternately for $\overline{\rho}_e < \overline{\rho}_i$ and $V_f > 0$, there is a gain of freshwater equivalent to an export situation.

# 4 Evaluation of parameters and data processing

Equation (10) contains $V_i$ (implicitly) and $V_e$, which are the volumes of water imported and exported by the tidal channel during the flood and the ebb, respectively. $V_i$ is obtained by integrating $v(t)$ (cf. (2)) from the time of low tide $t_{lo}$ through the ensuing time of high tide $t_{hi}$,

$$V_i = \int_{t_{lo}}^{t_{hi}} v(t)\ dt. \tag{11}$$

In the same way, the export volume reads as

$$V_e = \int_{t_{hi}}^{t_{lo^+}} v(t)\ dt, \tag{12}$$

where $t_{lo^+}$ is the time of the subsequent low tide. Although $V_i$ is not explicitly required by (10), it is necessary for the calculation of the volume-weighted mean potential density

$$\overline{\rho}_i = \frac{1}{V_i} \int_{t_{lo}}^{t_{hi}} \rho_{S,0,0}\ v(t)\ dt. \tag{13}$$

By analogy, the mean potential density for the exported water mass reads

$$\overline{\rho}_e = \frac{1}{V_e} \int_{t_{hi}}^{t_{lo^+}} \rho_{S,0,0}\ v(t)\ dt. \tag{14}$$

(Note that the two equations above are identical to equation (3) of Ridd et al. (1997), if density is substituted by salinity). The notation $\rho_{S,0,0}$ means that the potential density is calculated for the actual salinity measured at the pole, 0°C, and atmospheric pressure. Before applying equations (11)–(14) and finally equation (10), the basic time series of salinity and velocity were carefully inspected and pre-processed as follows:

- Only that data were used, where both salinity and velocity were well-defined at the same instant.
- In order to fill data gaps, the data were interpolated on a continuous time coordinate in 10-minute intervals (i.e. the original sampling interval) using cubic splines. This procedure works well for gaps smaller than a quarter-tide, but it fails for larger gaps. For large gaps, the interpolated data were removed.

- From the remaining data, only full tidal cycles were retained between two successive low water slacks; this yields 406 full tidal cycles. The water slacks were identified by the zero-crossings of the ADCP velocity. In cases where the zero-crossing was not well-defined, the velocity data were manipulated manually, but this concerned only 14 of the 812 zero-crossings.

- The "clean" tidal cycles were separated in half-tides for flood ($u >= 0$) and ebb ($u < 0$).

Now, $V_i$ and $\overline{\rho}_i$ were calculated for each flood cycle, $V_e$ and $\overline{\rho}_e$ for each ebb cycle, and finally the freshwater budget for each full cycle was evaluated according to equation (10).

# 5 Results

## 5.1 Tidal variability

For 2004, the time series of the tidal freshwater budget $V_f$, presuming $\epsilon_1 = \epsilon_2 \equiv 0$, is shown in Fig. 3a. The large data gaps in late May/early June and late September/early October are due to a malfunction of the ADCP, the smaller gaps were caused by blocking of the conductivity cell. $V_f$ exhibits high-frequency oscillations, the period of which is exactly two tidal periods. This behaviour is demonstrated in Fig. 4, which shows the $V_f$ time series for early April together with the water level. Except for the time before April 5 and after 15, $V_f$ follows clearly a zig-zag pattern.

Suspecting that this oscillatory behaviour is related to day and night tides, $V_f$ is displayed as a function of the high tide time $t_{hi}$ in Fig. 5, where $t_{hi}$ is assumed to be the central time of any tidal cycle. The contour plot shows that $V_f$ is highly variable, but there is some indication that the freshwater budget is negative for 12h $< t_{hi} <$ 24h, except for late June, July, late August, and late September/early October.

## 5.2 Seasonal variability

In Fig. 3a, the budget appears to be negative for most of the observational period, although the climate is assumed to be humid ($\mathcal{P} - \mathcal{E} > 0$) at this latitude. This impression is confirmed by the cumulative budget $V_f^c$ (Fig. 3b); the overall trend of the latter is negative, hence the Hörnum Basin is importing water on average, i.e. the water loss by evaporation is overcompensating the gain by precipitation and land runoff. Except for some short events, the slope of $V_f^c$ is positive only between middle of June and middle of July and in the middle of August. These "wet" periods stand out in Fig. 3c. Here, $\overline{V}_f$ is displayed which is derived from $V_f$ by application of a moving average with a window width of one month (about 27 days). These wet periods last for about five weeks in June/July and three weeks in August.

A negative budget means $\overline{\rho}_i < \overline{\rho}_e$ (see above) or, because thermal variations are excluded, the volume-weighted mean salinity of the ebb flow is higher than that during flood. For validation, the difference $\overline{\Delta s} = \overline{s}_i - \overline{s}_e$ between the mean salinity during flood and ebb, respectively was evaluated and again averaged over one month (the black curve in Fig. 3c). This curve is almost perfectly correlated with $\overline{V}_f$, indicating that during a negative budget the ebb flow is saltier. Note that no volume weighting was applied to the evaluation of $\overline{s}_i$ and $\overline{s}_e$ — with volume weighting, the curves would match exactly. Hence,

it is possible to determine the sign of the budget solely from the difference of the mean salinities during flood and ebb.

A pronounced seasonal cycle is visible, with negative budgets in spring and autumn and a positive budget in summer. In order to show whether this behaviour is typical for any year, the tidal budget $V_f$ was evaluated for years 2002 – 2006, and then averaged over the years using the same calibration for the volume flux in equation (2). This is somewhat critical, because the pole was dismantled every year in winter and re-erected in spring. Therefore, the position might have been varied from year to year by some tens of metres due to the inaccuracy of the positioning, and the distance of the ADCP from the bottom could be different by some tens of centimetres. However, the consequences for the volume flux calculation are assumed to be small. In the worst case, the value of the volume flux may be wrong, but the sign should be correct. As the budget averaged over the years is rather noisy, it was again averaged over one month yielding $\overline{V}_f^{seas}$ (Fig. 6). The freshwater budget is minimum in spring and autumn and maximum in summer.

### 5.3 Interannual variability

Fig. 7 shows that $\overline{V}_f$ exhibits a strong year-to-year variability. While for 2002 it is mostly negative, it is both negative and positive for 2003–2005 and largely positive for 2006. This is also reflected by the tidal mean budgets

$$\overline{V}_f^t = \frac{1}{N} \sum_1^N V_f(t), \tag{15}$$

given in the legend of Fig. 7, where $N$ is the number of tides within the observational period each year. $\overline{V}_f^t$ is negative for all years 2002 – 2005, and positive only in 2006. For 2003, 2004, and 2005 the budgets are almost identical.

## 6 Discussion

Regarding different scales of variability, the major findings emerged from the above results:

- the tidal freshwater budget of the Hörnum Basin oscillated with a period twice the tidal period,
- the seasonal freshwater budget exhibited a maximum in summer and was significantly correlated with the rainfall at the nearby meteorological stations, and
- for four out of five years analysed, the mean freshwater budget was negative.

While the second item demonstrates the consistency of observations and analyses, the other findings are unexpected and discussed in terms of the tidal and seasonal variability. The discussion is also supported by presenting the results of a very recent validation experiment.

### 6.1 Tidal variability

The potential candidates for triggering the quasi-diurnal cycle of $V_f$ are evaporation and the daily inequality of the tides; precipitation can be excluded at the outset because a diurnal cycle is not typical for moderate latitudes. The riverine land runoff is excluded as

well. It is controlled by sluices, the gates of which commonly open automatically during ebb tide, but this would generate a signal with a tidal period. Moreover, during drought periods the sluices are frequently closed for weeks or even months.

According to the bulk formula (cf. Gill, 1982, page 30), the evaporation rate over the ocean is proportional to the air density, the wind speed and the difference between the saturation specific humidity at the sea surface at sea surface temperature and the standard observation level. None of these parameters is known to exhibit a diurnal cycle. However, the bulk formula holds only for the open ocean and cannot be applied for a tidal basin, because open ocean conditions exist only when the tidal flats are submerged. Hence, if evaporation controls the two-tidal cycle of the freshwater budget, this can only be due to the different thermodynamic behaviour of the tidal flats when being dry around low tide.

From Andrews (1976, 1980) it is known that during low tide the skin temperature of the sediment may heat up to more than 20°C; recent observations of Onken et al. (2009) in the Hörnum tidal basin exhibit temperatures exceeding 30°C. As the sediment is wet and frequently covered by a thin water layer (ponds), the high temperatures are attained by the water in the ponds. As a consequence, the saturation specific humidity at the "sea surface" and the difference between the saturation specific humidity at the sea surface and the standard observation level (usually 10 m) increases exponentially, leading to strongly enhanced evaporation.

The starting point for a simple working hypothesis is that the dry tidal flats are heated during daylight hours. Due to the higher soil temperature of the flats, the evaporation is maximum during this time, leaving behind relatively salty water on the flats. During the flood, the water flushes the flats and takes up the high salinity water. As the limits for a tidal cycle are defined by the times of low tide, $t_{lo}$ and $t_{lo}^{+}$, the freshwater budget of the actual tidal cycle therefore depends on the preconditioning of the flats which took place six hours before $t_{hi}$.

Recalling Figs. 4 and 5, the two cases of $V_f < 0$ and $V_f > 0$ are discussed in terms of the above hypothesis:

- Case 1: $V_f < 0$
  This is frequently the case when the high tide is between about noon and midnight, when the preconditioning (i.e. enhanced evaporation) takes place within the time span from 6h through 18h when the flats are dry. Preconditioning occurs during daylight and enhanced evaporation is likely.

- Case 2: $V_f > 0$
  $V_f$ appears largely positive for high tides between midnight and noon, corresponding to dry flats from 18h through 6h. Preconditioning occurs at night and enhanced evaporation is unlikely.

The sign change of $V_f$ is thus in rough agreement with the hypothesis of enhanced evaporation on dry tidal flats during daylight hours. This is in agreement with the findings of Hollins and Ridd (1997), although their observations were done on a tidal flat in the tropics.

Sometimes however, predominantly in spring and autumn, $V_f$ is negative throughout the day regardless of the time of high tide. By contrast in summer, $V_f$ is frequently positive. One is tempted to assume that this "wet" time span is related to precipitation. In Fig. 8a are shown $V_f$ (cf. Fig. 3a) and the 2004 daily precipitation, averaged between the recording stations of Westerland which lies at about 15 km northwest of the pole and

Klanxbüll ($\approx$ 17 km northeast of the pole, cf. Fig. 1). Frequently, a similarity between the two quantities is evident. Sometimes, however, there is heavy precipitation (e.g. in the second half of July and in September), but no corresponding signal in the freshwater budget and vice versa, e.g. in late May and early July. This is probably due to the rather large distance between the pole and the weather stations or just the effect of local showers or thunderstorms. One must also take into account that a fraction of the rainfall, i.e. that over the sea, is detected immediately by the pole, while another fraction occurring over land, has a delayed impact on the freshwater budget, the timescale of which is unknown.

In search of a proxy that is representative of excessive evaporation, data from the short-wave radiation sensor mounted on top of the pole were analysed and related to the tidal freshwater budget. The integral radiation $I_R$ over ten minutes at the beginning of each tidal cycle was plotted together with the negative freshwater budget $-V_f$ in Fig. 8b. The maxima of $-V_f$ and $I_R$ are well correlated. Figure 8c shows a cut-out from 8b for the month of August. This supports the hypothesis that the tidal freshwater budget is controlled by excess of evaporation when the tidal flats are dry during daylight hours. A statistical evaluation (Fig. 8d) of the coincidence of the maxima accentuates the relationship: in 2004, the time series of $-V_f$ based on 406 tidal cycles exhibits 154 (out of 203 possible) maxima, the corresponding time series of $I_R$ has 189 maxima. From the latter, 122 maxima are correlated with maxima of $-V_f$. Hence, the relationship of maximum $-V_f$ and maximum solar radiation holds in 122 out of 154 cases, equivalent to a coincidence of 79%. Also the magnitude of $V_f$ depends on $I_R$, Though the correlation coefficient is only 0.32, the statistical p-value is less than 0.05 indicating significance. Hence, although $I_R$ was taken only over ten minutes during low tide, a high $I_R$ value indicates enhanced evaporation during the subsequent tidal cycle.

Motivated by the above results and in order to validate the working hypothesis that the evaporation over dry tidal flats is significantly higher than over wet tidelands, a simple experiment was conducted in the Jade estuary (located roughly 100 km south of the Hörnum Basin, see Fig. 1) in July 2008: containers made of acrylic glass were placed on the bottom of a shallow pond and filled with the ambient water. At this instant, the temperature and conductivity of the encased water volume were recorded, and once again after a couple of hours. Finally, the loss of freshwater due to evaporation was evaluated from the salinity change. One experiment took place on a calm and sunny day between 9:00h and 12:35h (local time) on July 24. While the mean water temperature within that period of time recorded at another pole located 300 m south in a tidal channel was about 17.5°C, the water temperature in the pond increased to 27.7°C, and the salinity from 32.10 to 32.75. The latter is equivalent to a freshwater loss of 0.96 mm. For comparison, the freshwater loss at the pole computed from the bulk parametrisation of Fairell et al. (1996) was only $9.4 \times 10^{-3}$ mm over the same period of time. This result supports the hypothesis that during daylight hours the evaporation on dry tidal flats is many times higher than in the neighbouring tidal channels or when the flats are submerged. Under favourable conditions (strong solar heating, large temperature difference between the ponds and the air, high wind speed, low relative humidity) this ratio may reach or even exceed two orders of magnitude.

As the daily inequality of the tides has not yet been discussed as a candidate triggering the quasi-diurnal cycle of the freshwater budget, the volume weighted mean potential density $\overline{\rho}_i$ (cf. (13)) was correlated with $V_f$. The idea behind this is that the inequality creates a variation in salinity at the position of the pole, because a higher tide requires enhanced advection of water from the North Sea with increased salinity, which is equivalent to increased potential density. Fig. 9 shows that $V_f$ is significantly correlated with

$\overline{p}_i$. In terms of the previous findings concerning the evaporation, this makes sense because enhanced advection of more saline water leads to a higher water level and at the same time to a shorter dry-falling period and less evaporation. However, the correlation of other potential parameters serving as proxies for the daily inequality, like the high tide water level or the difference between the levels of successive high and low tides, exhibit a much lower correlation. No correlation at all was found between the imported water volume $V_i$ and $V_f$. Hence, it is not clear to the authors to what degree the daily inequality of the tides controls the double-tidal period of the freshwater budget.

## 6.2 Seasonal variability

Excessive loss of freshwater appears to be a common feature for the Hörnum Basin. Dividing the numbers in the legend of Fig. 7 by the size of the catchment area, one obtains the mean loss during one tidal period in terms of the height of the water column. From a very recent Lagrangian drifter experiment in summer 2009, the size of the catchment area was set to 150 km$^2$, which is about four times the value derived from a Lagrangian model study and used in OCVR07. The corresponding daily water losses (assuming 0.52 tides per day) are 5.4 mm/day for 2002, 1.8 mm/day for 2003–2005, and the gain for 2006 is 0.5 mm/day, or a loss of about 2 mm/day averaged over all years. As the mean annual precipitation at Westerland and Klanxbüll is about 770 mm/year equivalent to 2 mm/day, the difference between the gain and the losses yields 4 mm/day which is attributed to evaporation. The latter number appears reasonable because the validation experiment above has demonstrated that already under moderate external conditions (7.5°C difference between air temperature and water temperature in the pond, light wind, shallow sandbank) an evaporation loss of 1 mm within 3.5 hours may be achieved. In case of higher flats, the dry-falling period will be longer, the solar heating on mudflats is more intense than on sandbanks, and in spring and autumn because of the lower air temperature the temperature difference will be larger. This number is also in agreement with those from previous studies. While for tropical (Hollins and Ridd, 1997; Hughes et al., 2001; Ridd et al., 1997; Wolanski and Ridd, 1986) and moderate latitudes (Acreman et al., 2003; Heath, 1977) mean evaporation rates between 2 mm/day and 3 mm/day were obtained, the study of Rouse et al. (1992) yields 4 mm/day for high subarctic conditions. Hence, a mean evaporation loss of 4 mm/day appears to be realistic.

In order to find out why the 2006 budget is different from those of previous years, $\overline{V}_f$ of each year was correlated within the observational period with time series of the parameters controlling the budget. These are the wind speed, the specific humidity at the standard level, and the saturation specific humidity at sea surface temperature. Additional parameters are the observed precipitation, and the land runoff. Unfortunately, the specific humidity at the standard level and the land runoff were not available. The results of the remaining calculations were mixed and difficult to interpret: while the sea surface temperature as a representative for the saturation specific humidity was positively correlated with the budget in 2002, 2003, 2005, and 2006 (correlation coefficients between .5 and .8), the correlation for 2004 was negative. The correlation of the wind speed with $\overline{V}_f$ was generally low in 2002–2005, but in 2006 a negative correlation of close to -.9 was found. This strange behaviour may be due to the non-linearity of the bulk formula, but correlating the product of wind speed and sea surface temperature with $\overline{V}_f$ gave no significant result at all. In order to take account of the heating of the flats during low tide, $\overline{V}_f$ was correlated with the solar radiation as a proxy parameter, but this provided significant negative correlations only for 2003 and positive correlations for 2006. Com-

paring $\overline{V}_f$ with the precipitation at Westerland and Klanxbüll yields significant negative and positive correlations for 2003 and 2004 only, while no correlation was obtained for the other years. In summary, all attempts to establish a relationship between the freshwater budget and any of the potential control variables failed; and in those cases where a significant correlation was found for one year, it could not be validated for other years. The lack of correlation with precipitation supports the conjecture that precipitation events are masked by evaporation.

# 7 Summary and Conclusions

A method has been presented to calculate the freshwater budget of a tidal basin from single-point high-frequency measurements of water velocity and salinity in a tidal channel, in conjunction with a one-time calibration of the volume flux against the water velocity. The method is based on mass conservation: for a single tidal cycle and under the assumption that the trajectories of water parcels are reversible for flood and ebb, respectively, the freshwater mass budget is the difference between the imported mass of water during flood and the exported mass during ebb plus an unknown quantity expressing the different water levels of successive low tides. Postulating in addition conservation of volume allows an expression of the freshwater volume budget as a function of the exported water volume and the volume-weighted mean densities of the imported and exported volumes.

The method is applied to time series of an observation pole positioned in a tidal channel in the Hörnum Basin, which is located in the northern part of the German Wadden Sea. For the years 2002 – 2006, and constrained to data of spring, summer, and autumn, the freshwater budget is analysed with respect to the tidal, seasonal, and interannual variability.

- The variability on the tidal time scale is characterised by oscillations, the period of which is twice the tidal period and triggered by the sequence of day and night tides: when the low tide is at daylight, the budget exhibits a local minimum because of enhanced evaporation on the exposed tidal flats. By contrast, a local maximum of the budget is correlated with low tide in the night.

- Variability on the seasonal time scale is evident after averaging the budget over many years. The seasonal budget is maximum for summer and minimum for spring and autumn.

- During four out of five years, the annual budget was negative, i.e. the loss of freshwater due to evaporation was over-compensating the gain by precipitation and land runoff. The mean daily loss is estimated as 4 mm.

The present paper increases the knowledge on air-sea interaction processes over the tidelands. In terms of the latent heat flux, it is shown that the common bulk parametrisations fail because they do not take account of the heating of the tidal flats during daylight hours. It will be a future task to extend the observations of the sediment temperature on the flats over the whole year, and to derive a more adequate bulk formula for the fluxes of latent and sensible heat over the tidelands. This will certainly improve the quality of local weather forecasts for the coastal zone.

# Acknowledgments

The authors greatly appreciate the engagement of Horst Garbe, Michael Janik, and Peter Kalensee for the maintenance of the observation poles and during field campaigns. We also thank the crew of *RV Ludwig Prandtl* for their help to deploy and recover the pole year by year, and the *Landesbetrieb Küstenschutz, Nationalpark und Meeresschutz Schleswig-Holstein* for the financial support. Precipitation data were obtained from the *Deutscher Wetterdienst* (DWD) in Offenbach (Germany).

# References


**Acreman, M.C, R.J. Harding, C.R. Lloyd, and D.D. McNeil** (2003), Evaporation characteristics of wetlands: experience from a wet grassland and a reed bed using eddy correlation methods. *Hydrology and Earth System Sciences*, 7, 1, 11–21.

**Andrews, R.** (1976) Wärmehaushaltsuntersuchungen im Wattgebiet der Nordseeküste (Heat balance investigations on the tidal flats on the North Sea coast). *Deutsche Gewässerkundliche Mitteilungen*, 20, 5, 117–126.

**Andrews, R.** (1980) Wärmeaustausch zwischen Wasser und Wattboden (Heat exchange between water and tidal flats). *Deutsche Gewässerkundliche Mitteilungen*, 24, 2, 57–65.

**Dietrich, G., K. Kalle, W. Krauss, and G. Siedler** (1980) *General Oceanography*, Wiley-Interscience, New York, 626 pp.

**Fairall, C.W.**, E.F. Bradley, D.P. Rogers, J.B. Edson, and G.S. Young (1996) Bulk parameterization of air-sea fluxes for Tropical Ocean-Global Atmosphere Coupled Ocean-Atmosphere Response Experiment. *Journal of Geophysical Research*, **101**, C2, 37747–3764.

**Gill, A.E.** (1982) *Atmosphere-Ocean Dynamics*, Academic Press, New York, 662 pp.

**Heath, R.A.** (1977) Heat balance in a small coastal inlet, Pauatahanui inlet, North island, New Zealand. *Estuarine and Coastal Marine Science*, 5, 783–792.

**Hollins, S., and P.V. Ridd** (1997) Evaporation over a tropical tidal salt flat. *Mangroves and Salt Marshes*, 1, 95–102.

**Hughes, C.E., J.D. Kalma, P. Binning, G.R. Willgoose, and M. Vertzonis** (2001) Estimating evapotranspiration for a temperate salt marsh, Newcastle, Australia. *Hydrological Processes*, 15, 957–975.

**Onken, R.**, U. Callies, B. Vaessen, and R. Riethmüller (2007) Indirect determination of the heat budget of tidal flats. *Continental Shelf Research*, **27**, 12, 1656–1676.

**Onken, R.**, Garbe, H., Schröder, S, and Janik, M. (2009) A new instrument for sediment temperature measurements. *IEEE Journal of Oceanic Engineering* (submitted).

**Neunhäuserer, L.**, B. Fay, and M. Raschendorfer (2007) Towards urbanisation of the non-hydrostatic numerical weather prediction model Lokalmodell (LM). *Boundary-Layer Meteorology*, **124**, 1, 81–97, doi 10.1007/s10546-007-9159-8

**Ridd, P., R. Sam, S. Hollins, and G. Brunskill** (1997) Water, salt and nutrient fluxes of tropical tidal salt flats. *Mangroves and Salt Marshes*, 1, 229–238.

**Ross, J., E. Mittelstaedt, H. Klein, R. Berger, and K. Ricklefs** (1998) Der Wasseraustausch im Tidebecken Hörnum-Tief. *Berichte des Bundesamtes für Seeschifffahrt und Hydrography*, 16, Hamburg and Rostock (Germany), 100 pp.

**Rouse, W.R, D.W. Carlson, and E.J. Weick** (1992) Impacts of summer warming on the energy and water balance of wetland tundra. *Climatic Change*, 22, 305–326.

**Wolanski, E., and P. Ridd** (1986) Tidal mixing and trapping in mangrove swamps. *Estuarine, Coastal and Shelf Science*, 23, 759–771.

# Glossary

| symbol | meaning | units |
|---|---|---|
| $a_0$ | calibration coefficient | $m^3 s^{-1}$ |
| $a_1$ | calibration coefficient | $m^2$ |
| $\mathcal{E}$ | freshwater loss/gain due to evaporation and condensation | kg |
| $\epsilon$ | uncertainty | kg |
| $\mathcal{F}$ | freshwater loss due to freezing of seawater | kg |
| $\mathcal{I}$ | freshwater gain due to inflow | kg |
| $I_R$ | irradiance | W $m^{-2}$ |
| *lhs* | left–hand side | |
| $\mathcal{M}$ | freshwater gain due to melting of ice | kg |
| $M$ | mass | kg |
| $M_e$ | exported mass of seawater during flood | kg |
| $M_f$ | freshwater mass due to land runoff, precipitation, evaporation, and condensation | kg |
| $M_i$ | imported mass of seawater during flood | kg |
| $\mathcal{O}$ | freshwater loss due to outflow | kg |
| $\mathcal{P}$ | freshwater gain due to precipitation | kg |
| $P$ | precipitation | mm $day^{-1}$ |
| $\mathcal{R}$ | freshwater gain due to land runoff and groundwater entry | kg |
| $\rho$ | density | kg $m^{-3}$ |
| $\overline{\rho}$ | volume-weighted mean density | kg $m^{-3}$ |
| *rhs* | right–hand side | |
| $s$ | salinity | |
| $s_e$ | salinity of exported water volume | |
| $\overline{s}_e$ | mean salinity of exported water volume | |
| $s_i$ | salinity of imported water volume | |
| $\overline{s}_i$ | mean salinity of imported water volume | |
| $t$ | time | s |
| $t_{hi}$ | time of high tide | s |
| $t_{lo}$ | time of low tide | s |
| $t_{lo^+}$ | time of subsequent low tide | s |
| $u$ | eastward velocity | $ms^{-1}$ |
| $V_e$ | exported volume | $m^{-3}$ |
| $V_f$ | freshwater volume due to land runoff, precipitation, evaporation, and condensation | $m^{-3}$ |
| $V_f^c$ | cumulative $V_f$ | $m^{-3}$ |
| $\overline{V_f}$ | $V_f$ averaged over one tropical month | $m^{-3}$ |
| $\overline{V_f}^d$ | daily mean $V_f$ | $m^{-3}$ |
| $\overline{V_f}^{seas}$ | $V_f$ averaged over one tropical month and over several years | $m^{-3}$ |
| $V_i$ | imported volume | $m^{-3}$ |
| $v$ | volume flux | $m^3 s^{-1}$ |

# List of Figures

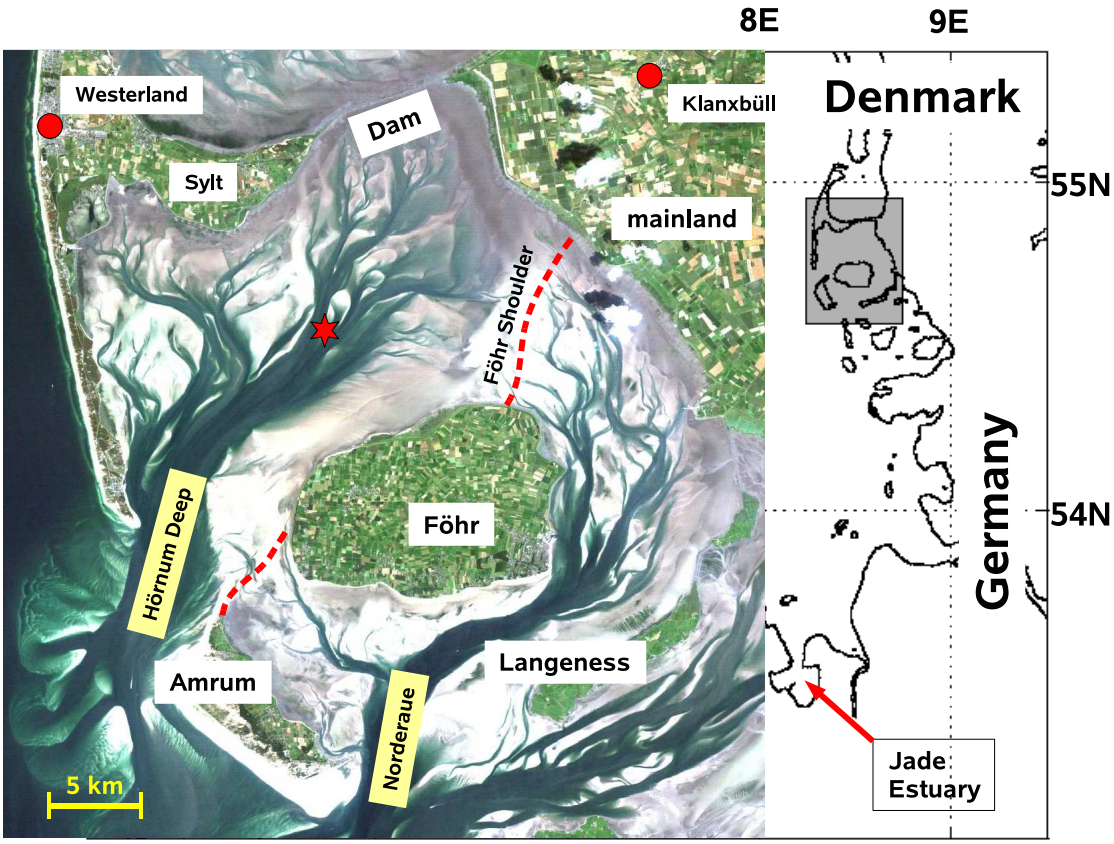


Figure 1: Satellite image of the Hörnum tidal basin at low tide; the red dashed lines indicate the approximate locations of the water sheds, i.e. the highest elevation of the topography between neighbouring tidal basins. The position of the observation pole is shown by the red asterisk. The geographical location of the basin is indicated by the gray-shaded box on the right. The Jade estuary is referred to in the Discussion.

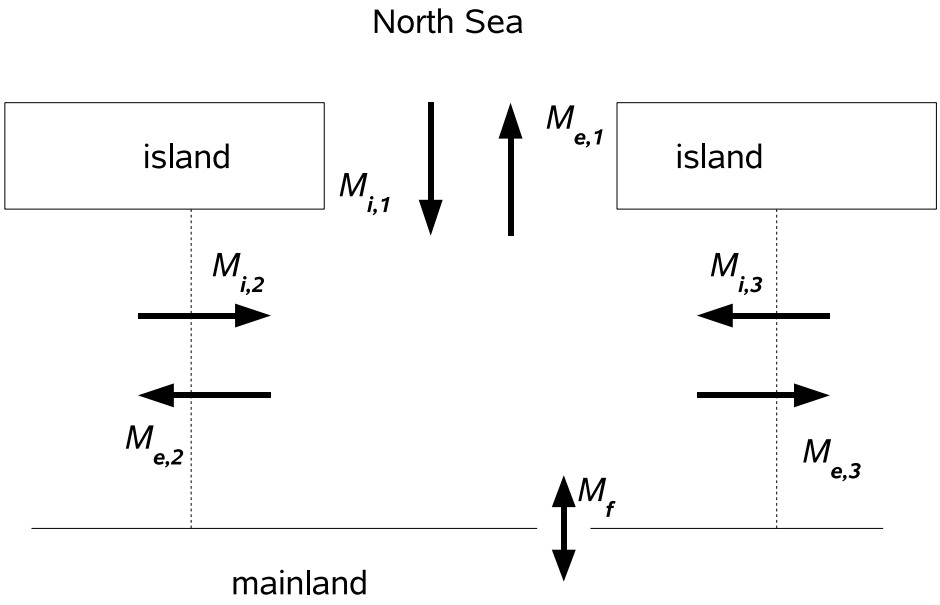


Figure 2: Components of the mass budget in an arbitrary tidal basin. Dashed lines indicate the water sheds.

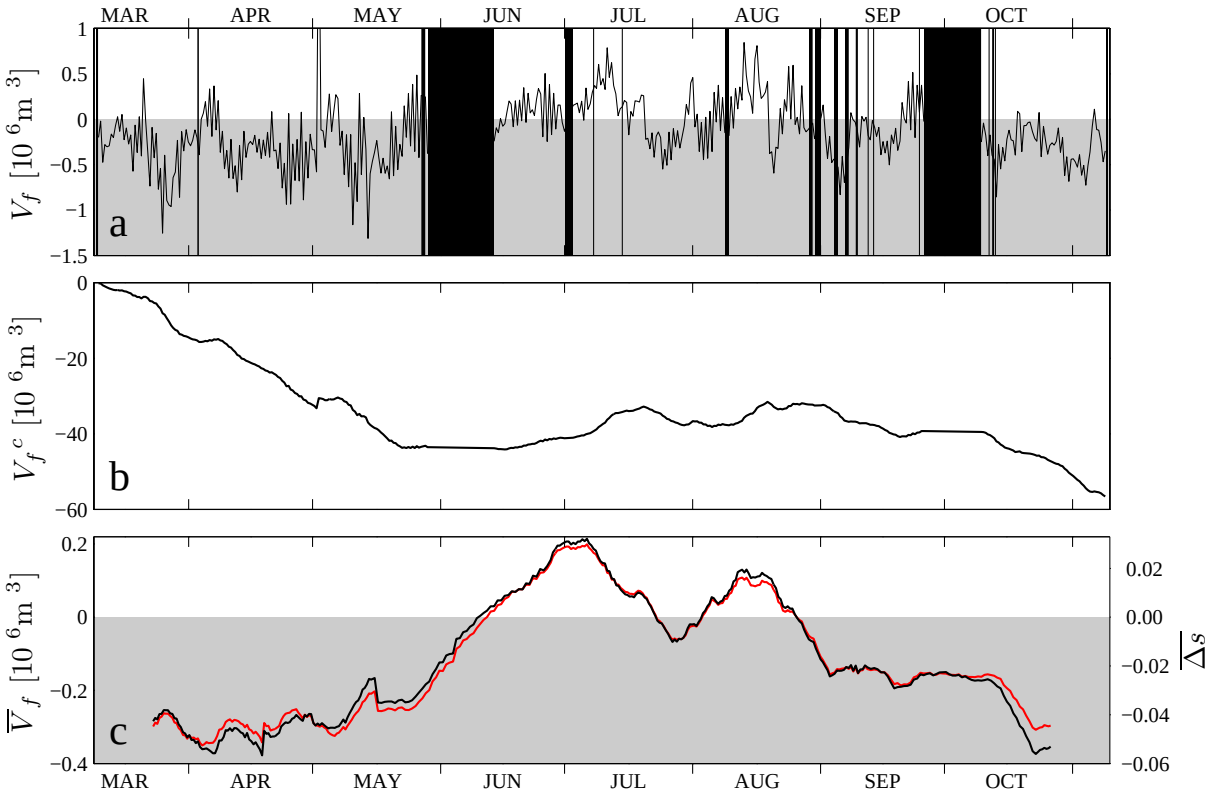


Figure 3: 2004 time series at the Hörnum pole: (a) freshwater budget; (b) cumulative freshwater budget; (c) mean freshwater budget running average over one month (red) and mean salinity difference between flood and ebb currents (black); negative ranges are grey-shaded in (a) and (c), missing data are indicated by black vertical bars in (a).

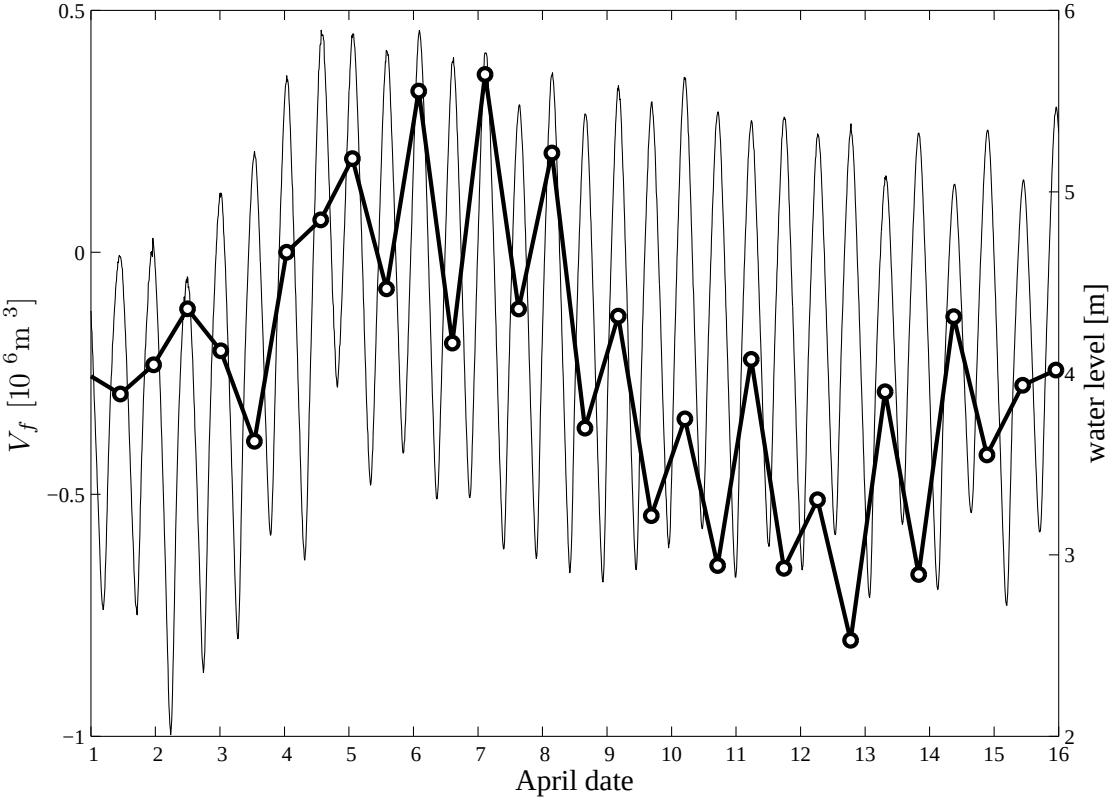


Figure 4: The freshwater flux $V_f$ (bold line) and the water level (thin line) in early April. The high water time $t_{hi}$ was selected as time coordinate for $V_f$, which was integrated between two low tides. The data points of $V_f$ are indicated by open circles.

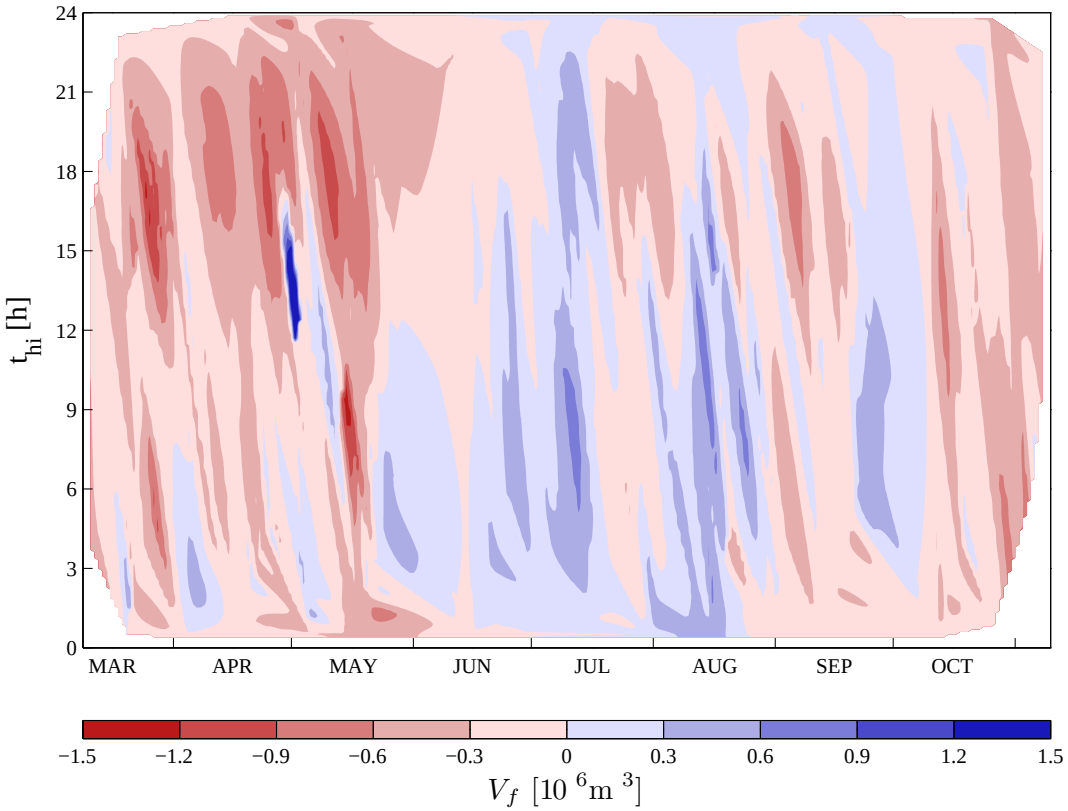


Figure 5: Contour plot of the 2004 tidal freshwater budget $V_f$ as a function of the date and local high tide time $t_{hi}$.

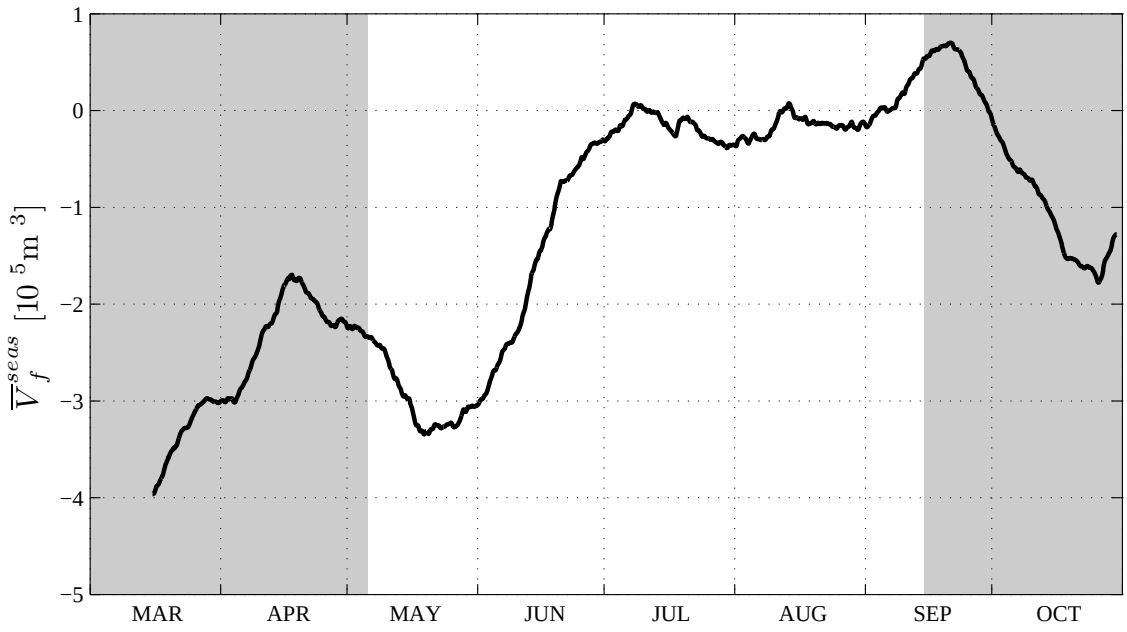


Figure 6: The seasonal freshwater budget $\overline{V}_f^{seas}$, averaged over the years 2002–2006 and over one tropical month. The highlighted area indicates the period of time where pole observations were available for each year.

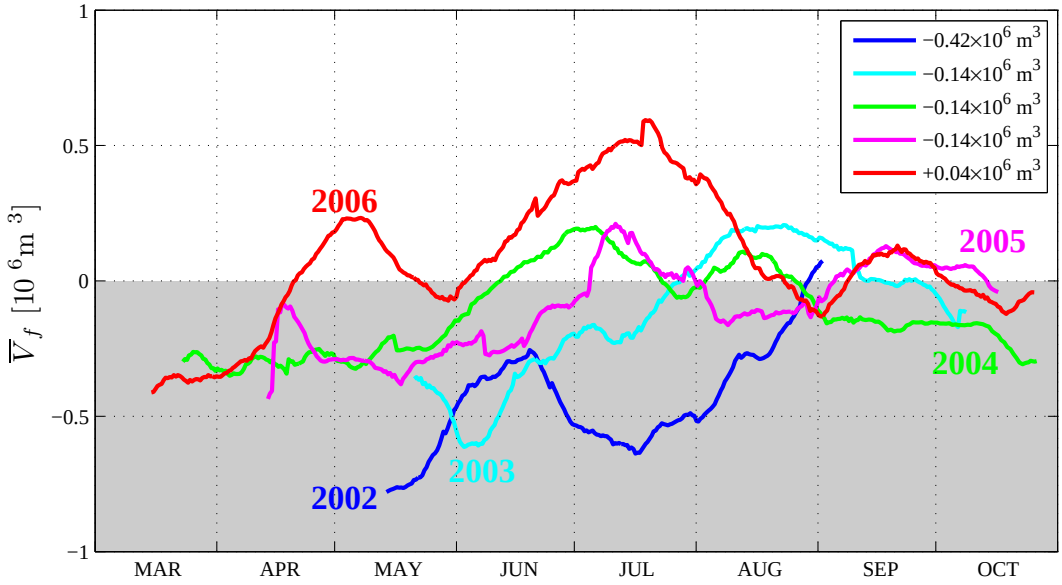


Figure 7: The mean freshwater budget $\overline{V}_f$ averaged over one tropical month, for the years 2002 – 2006. The numbers in the legend indicate the means for each year.

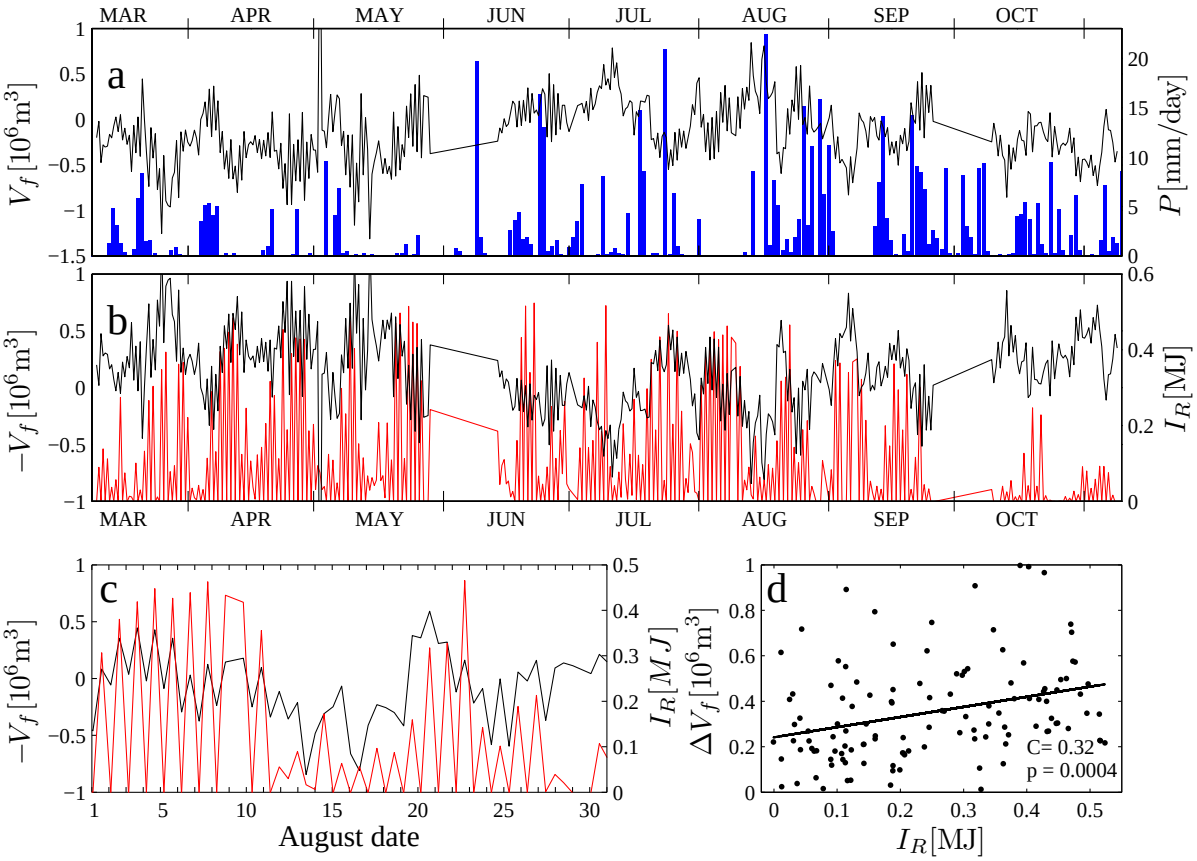


Figure 8: (a) The 2004 freshwater budget $V_f$ (solid line, cf. Fig. 3a) and daily average precipitation in Westerland and Klanxbüll (blue bars). (b) The negative freshwater budget $-V_f$ (black line) and the 10-minutes integral shortwave radiation $I_R$ (red line) at the time of low tide at the beginning of each tidal cycle. (c) same as (b) for the month of August, only. (d) $\Delta V_f$ vs. $I_R$ for matching maxima (for further explanation see text).

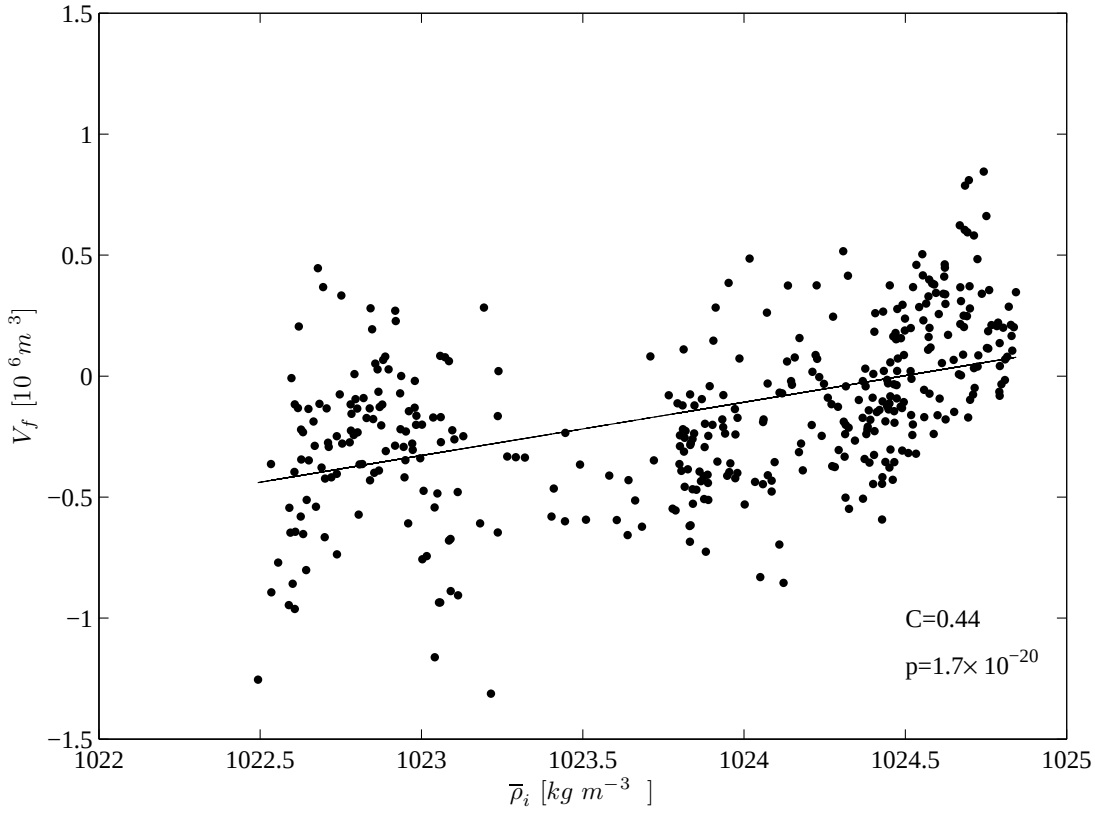


Figure 9: The freshwater budget $V_f$ vs. the volume weighted mean potential density $\overline{\rho}_i$ of the imported water volume at the pole in 2004. C and p are the correlation coefficient and the statistical p-value, respectively.